Effect of in-medium nucleon-nucleon cross section on proton-proton momentum correlation in intermediate-energy heavy-ion collisions

Ting-Ting Wang,[1,2] Yu-Gang Ma,[1,2,3,*] Chun-Jian Zhang,[1,2] and Zheng-Qiao Zhang[1,2]
[1]*Shanghai Institute of Applied Physics, Chinese Academy of Sciences, Shanghai 201800, China*
[2]*School of Physical Sciences, University of Chinese Academy of Sciences, Beijing 100049, China*
[3]*School of Physical Science and Technology, ShanghaiTech University, Shanghai 200031, China*

(Received 28 July 2017; published 23 March 2018)

The proton-proton momentum correlation function from different rapidity regions is systematically investigated for the Au + Au collisions at different impact parameters and different energies from 400*A* MeV to 1500*A* MeV in the framework of the isospin-dependent quantum molecular dynamics model complemented by the Lednický-Lyuboshitz analytical method. In particular, the in-medium nucleon-nucleon cross-section dependence of the correlation function is brought into focus, while the impact parameter and energy dependence of the momentum correlation function are also explored. The sizes of the emission source are extracted by fitting the momentum correlation functions using the Gaussian source method. We find that the in-medium nucleon-nucleon cross section obviously influences the proton-proton momentum correlation function, which is from the whole-rapidity or projectile or target rapidity region at smaller impact parameters, but there is no effect on the mid-rapidity proton-proton momentum correlation function, which indicates that the emission mechanism differs between projectile or target rapidity and mid-rapidity protons.

DOI: 10.1103/PhysRevC.97.034617

I. INTRODUCTION

The Hanbury Brown–Twiss (HBT) effect was first discussed in radio and stellar astronomy. The method was applied to measure the angular diameter and the size of stars by Hanbury Brown and Twiss [1]. Later on, the technique was introduced to research particle physics in the 1960s by Goldhaber *et al.* They studied the angular distribution of identical pion pairs in proton-antiproton annihilations and observed an enhancement of pairs at small relative momenta [2]. The past decade has brought great strides in experiments and a larger number of theoretical researches ranging from low-energy to high-energy Heavy-ion collisions (HICs) [3,4]. It is well known that two-particle correlation is sensitive to characteristics of the particle emission source. Recently, two-particle correlation in subatomic physics was taken as a probe for the space-time geometry of the particle emission source. The correlation between two protons was measured by several experiments and explored by different models. Not only protons but also the composite light fragments and particles, which are not discussed in this paper, are also used to carry information on the emission source [5,6]. Owing to the rapid development of radioactive nuclear beams, the HBT method is also used to study the exotic structure of nuclei. For instance, there have been several measurements for revealing the exotic structure of neutron-rich nuclei such as ^{6}He, ^{11}Li, and ^{14}Be [7–9] and of proton-rich nuclei such as ^{23}Al [10] as well as ^{22}Mg [11,12]. In addition, the dependence of the proton-neutron correlation on the binding energy was also theoretically explored [13]. In addition to the applications of the HBT method to investigate the exotic structure, it has become an important tool in heavy-ion collisions at wide energy ranges [3,4,14–16]. For example, in the relativistic energy region, the collaborations at the Relativistic Heavy Ion Collider and the Large Hadron Collider have carried out a lot of experimental measurements of the correlation function of two pions as a function of energy and system size [17,18]. What is more, the same method has been applied to make the first measurement of a two-antiproton interaction by analyzing the momentum correlation function between antiprotons, namely, the quantitative extraction of the scattering length and the effective range, which are two key parameters to characterize the strong interaction for the antiproton interactions by the STAR Collaboration [19–22]. Theoretically, the correlation functions between two identical pions or kaons were also investigated in some simulation work such as the hydrodynamic model and A Multiphase Transport model (AMPT) [4,23–27]. In the intermediate-energy region, the two-proton correlation functions were mostly applied to extract space-time properties such as the source size and emission time in the nuclear reaction [28]. In addition, there are many investigations of the dependencies of the correlation functions in the experiments and theories, such as on the impact parameter [29,30], the total momentum of nucleon pairs [31], the isospin of the emission source [32], the nuclear symmetry energy [33], the nuclear equation of state (EOS) [30], and the density distribution of valence neutrons in neutron-rich nuclei [6].

The investigation of in-medium nucleon-nucleon scattering is of interest in intermediate-energy heavy-ion reactions. In this energy domain, nucleus-nucleus collisions provide a unique opportunity to form compressed nuclear matter with a density

*Corresponding author: ygma@sinap.ac.cn

 ©2018 American Physical Society

up to two to three times normal nuclear matter density (ρ_0). The in-medium nucleon-nucleon cross section (NNCS) has a close relation with the nuclear matter density. Therefore, it is an important component in our model simulations. Recently, the medium effects on nucleon-nucleon cross sections have been widely investigated by replacing the NNCS in vacuum with an in-medium one and the various effects have been discussed [34–37].

The dependence of the two-proton correlation function on the in-medium NNCS has been briefly studied via the Correlation After Burner (CRAB) code in the framework of an isospin-dependent quantum molecular dynamics (IQMD) model [30]. Since the two-particle correlation function, through final-state interactions and quantum statistical effects, has been shown to be a sensitive probe to the space-time distributions of emitted particles in heavy-ion collisions [16], it is of great interest to investigate the in-medium nucleon-nucleon (*NN*) cross-section effects on the source evolution. In the present paper, we use another theoretical approach which was proposed by Lednický and Lyuboshitz [38] to explore the relationship between the above factors and proton-proton correlation function in more detail. The two-particle correlation at small relative velocities is sensitive to the space-time characteristics of the production process owing to the effects of quantum statistics and final-state interaction [39,40]. In most proton-proton correlation functions, the HBT strength at 20 MeV/c of the p-p relative momentum is taken as a unique quantity to determine the source size or emission time of two-proton emission [30]. The proton phase spaces of Au+Au collisions at the freeze-out time generated by the IQMD model are used as the input for the Lednický-Lyuboshitz code and then the effective source size of the source is extracted.

The rest of paper is organized as follows. In Sec. II we briefly describe the models and formalism used in the present study, i.e., the Lednický-Lyuboshitz analytical formalism and an IQMD model. The detailed analysis and discussion of a systematic proton-proton momentum correlation function (C_{pp}) and extracted source size results for different rapidity regions are given for different in-medium nucleon-nucleon cross sections, different impact parameters, and different beam energies for Au + Au collisions in Sec. III. In addition, we fit the proton p_T spectra with the distribution function from the blast-wave model and discuss the relationship between proton-proton correlation strength and radial flow velocity. Finally, in Sec. IV we summarize the results.

II. FORMALISM AND MODELS

A. Lednický-Lyuboshitz analytical formalism

First, we would like to present a brief review of the theoretical approach that was proposed by Lednický and Lyuboshitz [38] for the HBT analysis. The method is based on the principle that the correlation functions of identical particles when they are emitted at small relative momenta are determined by the effects of quantum-statistical symmetry (QS) of particles and the final-state interaction (FSI) [41]. In this technique, we assume that the particles emitted by an independent one-particle point source and the spin are independent in the production progress as well as the two-particle interaction. Then we can investigate particle pairs (1,2) emitted at small relative momenta. Owing to the conditions in Refs. [42], we neglect the effect of FSI in all pairs $(1,i)$ and $(2,i)$ except for (1,2). We can see the progress in Fig. 1.

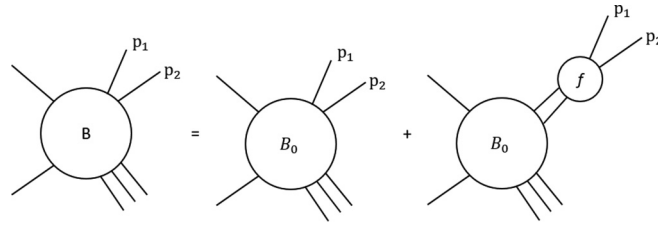

FIG. 1. Production of interacting particles 1 and 2 [42].

So the correlation function for identical particles takes the expression

$$B(\mathbf{p},\mathbf{q}) = B_0(\mathbf{p},\mathbf{q}) + B_1(\mathbf{p},\mathbf{q}), \tag{1}$$

where

$$\mathbf{p} = \mathbf{p}_1 + \mathbf{p}_2, \qquad \mathbf{q} = \tfrac{1}{2}|\mathbf{p}_2 - \mathbf{p}_1|, \tag{2}$$

are the total momentum and relative momentum of the particle pair, respectively. In Eq. (1), $B_0(\mathbf{p},\mathbf{q})$ is the contribution of the quantum statistics effect, described by the formula

$$B_0(\mathbf{p},\mathbf{q}) = g_0 \cos(\mathbf{qx}). \tag{3}$$

Here g_0 is the spin factor.

Then, the function $B_1(\mathbf{p},\mathbf{q})$ can be expressed through the symmetrized Bethe-Salpeter amplitude $\psi(S)$, which can be approximated by the outer region solution of the scattering problem [19]:

$$B_1(\mathbf{p},\mathbf{q}) = \sum_S \rho_{S,\mathbf{p}}(x_1,x_2,x_1',x_2') \times \psi^S_{\mathbf{p},\mathbf{q}}(x_1,x_2) \times \psi^S_{\mathbf{p},\mathbf{q}}(x_1',x_2') d^4x_1 d^4x_2 d^4x_1' d^4x_2', \tag{4}$$

where $\rho_{S,\mathbf{p}}$ is the two-particle density matrix.

Next, we can introduce the detailed analytical calculation of the proton-proton correlation function [19]. The proton-proton correlation function, $C_{pp}(\mathbf{k}^*,r_0)$, can be described by the Lednický-Lyuboshitz analytical method [19,38]. In this model, the space distribution of the Gaussian source was simulated according to the following function:

$$S(\mathbf{r}^*) \approx \exp\left(-\mathbf{r}^{*^2}/\left(4r_0^2\right)\right). \tag{5}$$

Here, r_0 is the source size parameter. Therefore, we can obtain the correlation function through assuming 1/4 of the singlet and 3/4 of triplet states. The theoretical correlation function at a given k^* can be calculated as the average FSI weight $\langle w(\mathbf{k}^*,\mathbf{r}^*)\rangle$ obtained from the separation r^*, simulated according to the Gaussian law, and the angle between the vectors $\mathbf{k}^*$ and $\mathbf{r}^*$, simulated according to a uniform cosine distribution. The average FSI weight can be described by the formula

$$w(\mathbf{k}^*,\mathbf{r}^*) = \left|\psi^{S(+)}_{-\mathbf{k}^*}(\mathbf{r}^*) + (-1)^S \psi^{S(+)}_{\mathbf{k}^*}(\mathbf{r}^*)\right|^2/2, \tag{6}$$

where S is the total pair spin, $\mathbf{r}^*$ is the relative distance, $\psi^{S(+)}_{-\mathbf{k}^*}(\mathbf{r}^*)$ is the equal-time ($t^* = 0$) reduced Bethe-Salpeter amplitude which can be approximated by the outer solution of the scattering problem [38]. This is

$$\psi^{S(+)}_{-\mathbf{k}^*}(\mathbf{r}^*) = e^{i\delta_c}\sqrt{A_c(\lambda)} \times\left[e^{-i\mathbf{k}^*\mathbf{r}^*}F(-i\lambda,1,i\xi) + f_c(k^*)\frac{\tilde{G}(\rho,\lambda)}{r^*}\right], \quad (7)$$

where $\delta_c = \arg\Gamma(1 + i/k^*a_c)$ is the Coulomb phase corresponding to zero orbital angular momentum, $A_c(\lambda) = 2\pi\lambda[\exp(2\pi\lambda) - 1]^{-1}$ determines the contribution of the Coulomb interaction, i.e., the positive value corresponding to the repulsion, $\lambda = (k^*a_c)^{-1}$, $a_c = 57.5$ fm is the Bohr radius for two protons, $\rho = k^*r^*$, $\xi = \mathbf{k}^*\mathbf{r}^* + \rho$, F is the confluent hypergeometric function, $\tilde{G}(\rho,\lambda) = \sqrt{A_c(\lambda)}[G_0(\rho,\lambda) + iF_0(\rho,\lambda)]$ is a combination of the regular (F_0) and singular (G_0) s-wave Coulomb function,

$$f_c(k^*) = \left[\frac{1}{f_0} + \frac{1}{2}d_0k^{*2} - \frac{2}{a_c}h(\lambda) - ik^*A_c(\lambda)\right]^{-1} \quad (8)$$

is the s-wave scattering amplitude renormalized by the Coulomb interaction, d_0 is the effective range of the interaction, and $h(\lambda) = \lambda^2\sum_{n=1}^{\infty}[n(n^2+\lambda^2)]^{-1} - C - \ln[\lambda]$ (here $C = 0.5772$ is the Euler constant). The dependence of the scattering parameters on the total pair spin S is omitted since only the singlet ($S = 0$) s-wave FSI contributes in the case of identical nucleons.

B. The IQMD model

To apply the above theoretical simulation, the single-particle phase-space distribution at the freeze-out is required. In this work, the correlation function can be established from the emission phase space given by the IQMD transport model [43].

The quantum molecular dynamics (QMD) model is a many-body transport theory; it has been extensively applied to describe heavy-ion reactions from intermediate energy to $2A$ GeV [44]. From the QMD studies, various valuable information about both the collision dynamics and the fragmentation process has been learned [45–54]. Excellent extensibility can be also expected due to its microscopic treatment of the collision process. The model mainly consists of several parts: initialization of the projectile and the target nucleons, nucleon transport under the effective potentials, NN binary collisions in a nuclear medium, Pauli blocking, and the numerical test. The IQMD model is based on the QMD model and considers the isospin factors [55] in mean-field, two-body NN collisions, and Pauli blocking. In the IQMD model, the wave function of each nucleon is represented by the form of the Gaussian wave packet, with the parameter L which relates to the size of the reaction system. For the Au + Au system, the width L is fixed to 2.16 fm^2. The Gaussian wave packet is written as

$$\phi_i(\mathbf{r}) = \frac{1}{2\pi L^3/4}\exp\left(\frac{-(\mathbf{r} - \mathbf{r}_i(t))^2}{4L}\right)\exp\left(\frac{i\mathbf{r}\cdot\mathbf{p}_i(t)}{\hbar}\right). \quad (9)$$

Here, $\mathbf{r}_i(t)$ and $\mathbf{p}_i(t)$ are the time-dependent variables which describe the center of the packet in coordinate and momentum space, respectively. Then, all nucleons interact via the effective mean-field and two-body NN collisions.

The nuclear mean field can be expressed as

$$U = U_{\rm Sky} + U_{\rm Coul} + U_{\rm Yuk} + U_{\rm sym} + U_{\rm MDI} + U_{\rm Pauli}, \quad (10)$$

where $U_{\rm Sky}$, $U_{\rm Coul}$, $U_{\rm Yuk}$, $U_{\rm sym}$, $U_{\rm MDI}$, and $U_{\rm Pauli}$ are the density-dependent Skyrme potential, the Coulomb potential, the surface Yukawa potential, the isospin asymmetry potential, the momentum-dependent interaction (MDI), and the Pauli potential, respectively. A general review of the above potentials can be found in Ref. [44]. In the present work, the in-medium NN cross section is represented by the formula

$$\sigma^{\rm med}_{NN} = \left(1 - \eta\frac{\rho}{\rho_0}\right)\sigma^{\rm free}_{NN}, \quad (11)$$

where ρ_0 is the normal nuclear matter density, ρ is the local density, η is the in-medium factor, and $\sigma^{\rm free}_{NN}$ is the available experimental NN cross section [56]. In this above expression, increasing values of the parameter η correspond to decreasing values of the in-medium nucleon-nucleon cross section.

In this model, the fragments are identified using a modified minimum spanning tree description. In the minimum spanning tree approach, two nucleons are assumed to share the same cluster if their centers are closer than a distance of 3.5 fm and their relative momentum smaller than 0.3 GeV/c. If a nucleon is not bounded by any clusters, it is treated by an emitted (free) nucleon.

C. The blast-wave fit

In heavy-ion collisions, particles collide with each other randomly, which can be described in terms of thermal motion [57]. We adopt the blast-wave model, which has been put forward by Siemens and Rasmussen [58] to describe the midrapidity p_T spectra with two free parameters: collective transverse flow velocity β and kinetic freeze-out temperature T_f. The collective transverse flow velocity β is parametrized by the surface velocity β_s in the region of $0 \leqslant R \leqslant R_{\rm max}$ [59]:

$$\beta_r(r) = \beta_s\left(\frac{r}{R_{\rm max}}\right)^{\alpha}, \quad (12)$$

where $R_{\rm max}$ is the maximum radius of the expanding source at thermal freeze-out time, β_s is the particle radial velocity at the maximum surface, e.g., $r = R_{\rm max}$, and the exponent α describes the evolution of the flow velocity with the radius. The p_T spectra are a superposition of individual thermal sources with different r, which is boosted with the boost angle $\rho = \tanh^{-1}\beta_r(r)$ [60,61].

$$\frac{dn}{p_T dp_T} \propto \int_0^{R_{\rm max}} r\,dr m_T I_0\left(\frac{p_T\sinh\rho}{T_f}\right)K_1\left(\frac{m_T\cosh\rho}{T_f}\right), \quad (13)$$

where K_1 and I_0 are the modified Bessel functions. The shapes of the spectra are essentially determined by T_f, β_S, α, and the mass of the particle, m_0. The average flow velocity is estimated by taking an average over the transverse geometry.

III. ANALYSIS AND DISCUSSION

In this work, we use the soft EOS with momentum-dependent interaction for all Au + Au collisions at beam energies from 0.4 to 1.5A GeV. The correlation functions are calculated by using the phase-space information from the freeze-out stage.

First, we investigate the influence of the in-medium NN cross section on the momentum correlation function for Au + Au collisions at 1.0A GeV. Figure 2 shows the proton-proton momentum correlation function for Au + Au collisions at 1A GeV with different in-medium reduction factors η, impact parameters, and proton rapidity region. In each panel, in-medium reduction factors of 0.0, 0.2, 0.5, 0.7, and 0.9 are compared. From top to bottom, each panel corresponds to different impact parameters, from $b = 3$, 6, 9, and up to 12 fm, respectively. From left to right, it represents the correlation function for the proton pairs within whole rapidity, mid-rapidity, and projectile or target rapidities, respectively. Here the mid-rapidity cut means that both protons are emitted in the rapidity window of $-0.5 \leqslant y/y_{\rm proj} \leqslant 0.5$, and the projectile or target rapidity region indicates that both protons come from the rapidity region of either $y/y_{\rm proj} \geqslant 0.5$ or $y/y_{\rm proj} \leqslant -0.5$, where y represents the proton rapidity and $y_{\rm proj}$ means the initial projectile rapidity. Overall, the proton-proton momentum correlation function exhibits a peak at relative momentum $q = 20\,{\rm MeV}/c$, which is due to the strong final-state s-wave attraction together with the suppression at lower relative momentum as a result of Coulomb repulsion and the antisymmetrization wave function between two protons.

For protons which are emitted in whole rapidity or projectile or target rapidity, the general trend is very similar. With the increasing of the in-medium NN cross section (i.e., the less in-medium reduction factor η), the collision rate between nucleons increases. Therefore, more nucleons are emitted early, which makes the strength of the momentum correlation function larger. The difference can be further revealed in central and semi-peripheral collisions; however, the difference in momentum correlation function among different η factors almost disappears in peripheral collisions. This indicates that the NN cross section in peripheral collisions has no significant change even though the η value changes much. Generally speaking, with less nucleon-nucleon cross section (i.e., larger η factor), the correlation peak decreases, indicating that proton-proton correlation has a positive correlation with nucleon-nucleon cross section. The sensitivity of correlation strength to the η values becomes less important when the reaction goes to peripheral collisions. For mid-rapidity protons, correlation functions are much stronger than the cases of whole rapidity or projectile or target rapidity, and show almost no dependence on the in-medium nucleon-nucleon cross section, which indicates

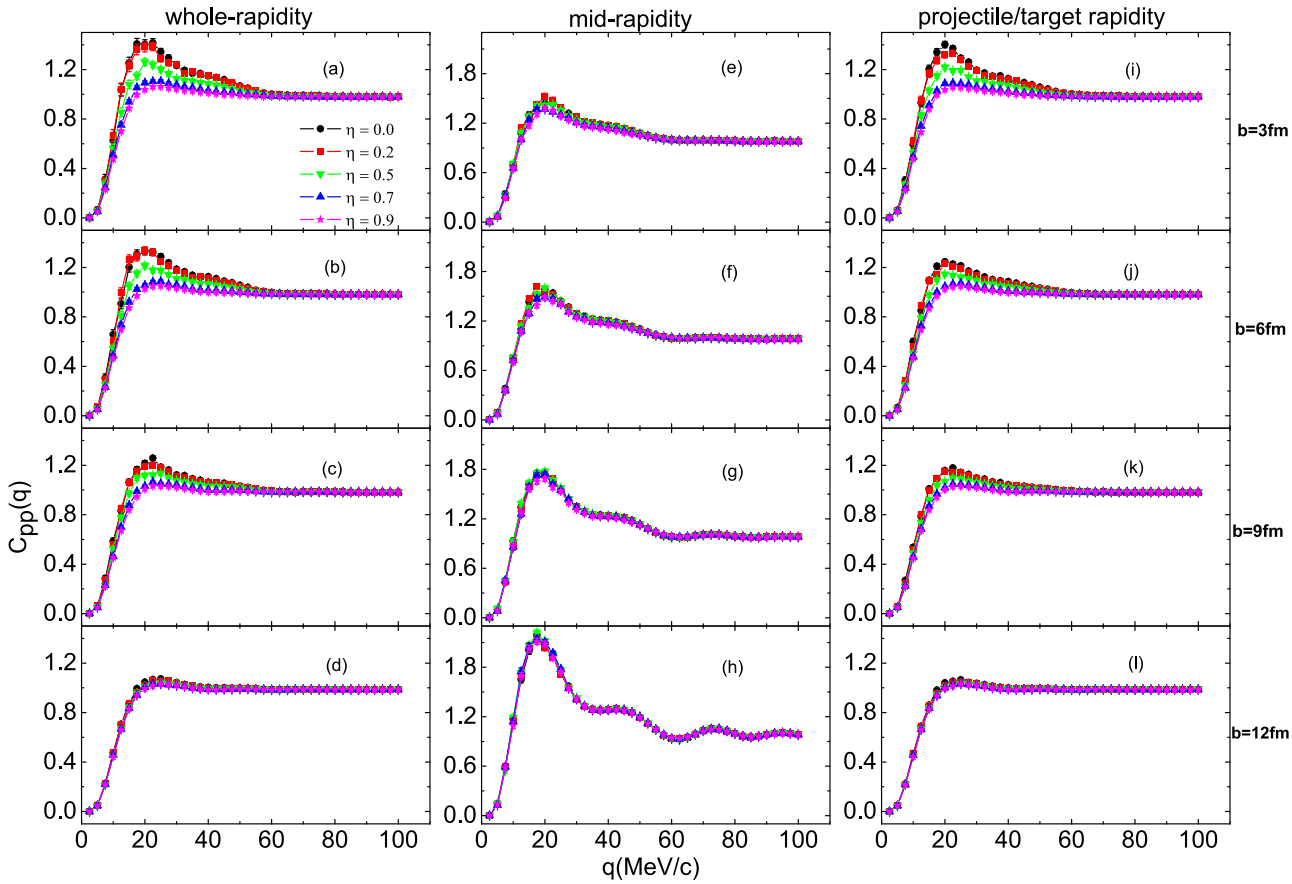

FIG. 2. Momentum correlation function of proton pairs for Au + Au collisions at 1A GeV with different in-medium reduction factors. From top to bottom, each panel corresponds to impact parameters, namely, $b = 3$, 6, 9 and 12 fm, respectively. From left to right, each panel represents the correlation function constructed for the proton pairs within whole rapidity, mid-rapidity and projectile or target rapidities, respectively.

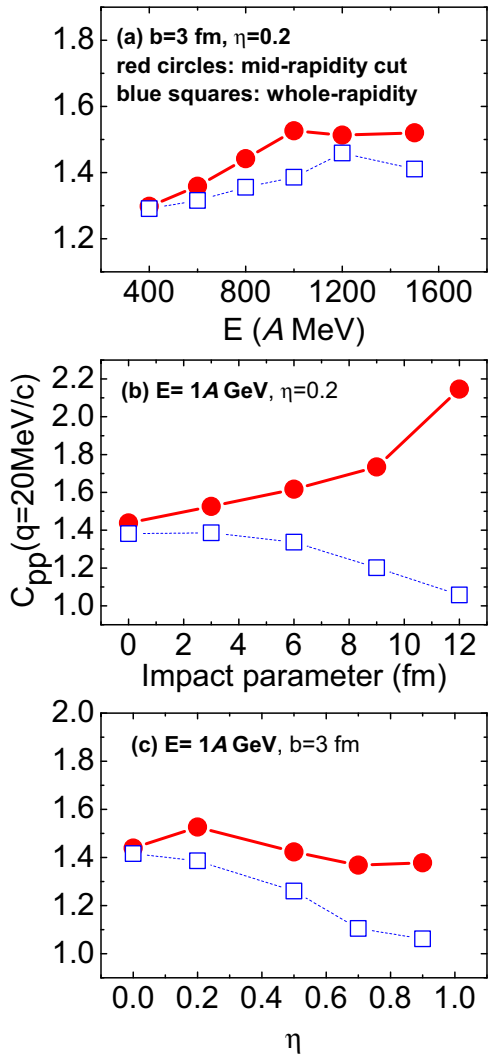

FIG. 3. (a) C_{pp} strength at 20 MeV/c as a function of the incident energy, which is calculated at an impact parameter of $b = 3$ fm and in-medium reduction factor of $\eta = 0.2$; (b) C_{pp} strength at 20 MeV/c as a function of the impact parameter, which is calculated at 1A GeV and the in-medium reduction factor $\eta = 0.2$; (c) C_{pp} strength at 20 MeV/c as a function of the in-medium reduction factor, which is calculated at $b = 3$ fm and 1A GeV. Note that the red circles correspond to the mid-rapidity cut and the blue squares to the whole-rapidity cut.

a very different space-time structure of mid-rapidity protons. Essentially, the mid-rapidity protons are emitted very early and at non-equilibrium, and are therefore insensitive to the in-medium NN cross section; additionally they have radial flow, which is mentioned later. In addition, another difference is that the strength of the correlation peak as a function of impact parameter is the reverse of the behavior of the correlation peak for whole rapidity or projectile or target rapidity protons, which displays a stronger correlation peak in peripheral collisions than central collisions, indicating a slightly more compact mid-rapidity source in peripheral collisions.

How the three variables of incident energy, impact parameter, and in-medium nucleon-nucleon cross section affect the strength of C_{pp} is presented in Fig. 3 for the proton-proton correlation function where the whole-rapidity window (blue squares) or mid-rapidity (solid circles) is applied for emitted protons in Au + Au collisions. For the incident energy dependence, the increase of momentum correlation peak from low energy to high energy is cleanly seen in Fig. 3(a), and the mid-rapidity cut displays a stronger peak. It can be generally understood that at higher energy, a more rapid collision process, and a smaller emission source space and short time interval among emitting nucleons in whole rapidity region, so does in the mid-rapidity nucleons [30]. In Fig. 3(b), we see that the correlation strength increases with the impact parameter for the mid-rapidity cut but the opposite occurs for the whole-rapidity cut, which shows that geometrical cuts for two rapidities are complemented; e.g., a stronger correlation for mid-rapidity protons at peripheral collision indicates smaller source size, but a weaker correlation for whole-rapidity protons indicates larger source size. In Fig. 3(c), with the increase of the in-medium cross-section modification factor, i.e., decreasing the in-medium NN cross section, the peak strength becomes smaller. In other words, proton-proton correlation positively depends on the nucleon-nucleon collisions. However, in contrast with the whole-rapidity protons, mid-rapidity protons show weaker sensitivity to the NNCS. Because we already know that the strength of the correlation function depends mainly on the source size, the above behavior of the HBT strength essentially reflects the changing size of the emission source versus the beam energy, impact parameter, and nucleon-nucleon cross section.

Figure 4 presents the radius of the Gaussian source for emitted protons as a function of beam energy (left column), impact parameter (middle column), and in-medium cross-section reduction factor (right column) for different rapidity windows, namely, the whole rapidity (upper row), mid-rapidity (middle row), and projectile or target rapidity (bottom row). Overall, for mid-rapidity proton-proton correlations, the sensitivity to the in-medium cross-section reduction factor is almost not visible. The source radius shows a slight drop with increase of beam energy or impact parameter. For the whole rapidity or projectile or target rapidity windows, their beam energy dependencies are very similar if the same η is applied, and the source radius increases with the increase of η, i.e., the decrease of nucleon-nucleon cross section. When the nucleon-nucleon cross section is larger (e.g., $\eta \leqslant 0.5$), the source radius drops with the incident energy, indicating fast emission and/or compact proton emission size in higher energies. However, the situation is different when the nucleon-nucleon cross section is small (e.g., $\eta > 0.7$), where the radius shows a slight increasing or a plateau behavior. But overall, even though a slight beam energy dependence of the radius is visible, the trend is rather weak as seen in ultra-relativistic energy heavy-ion collisions [62].

The middle and right-hand columns demonstrate the radius of the Gaussian source as a function of impact parameter at different fixed η values or η at different impact parameters, respectively. As expected, for correlation between protons from the whole rapidity region or the projectile or target region, the source size increases with the increasing of impact parameter, and the larger the nucleon-nucleon cross section, the stronger the dependence of the source size on impact

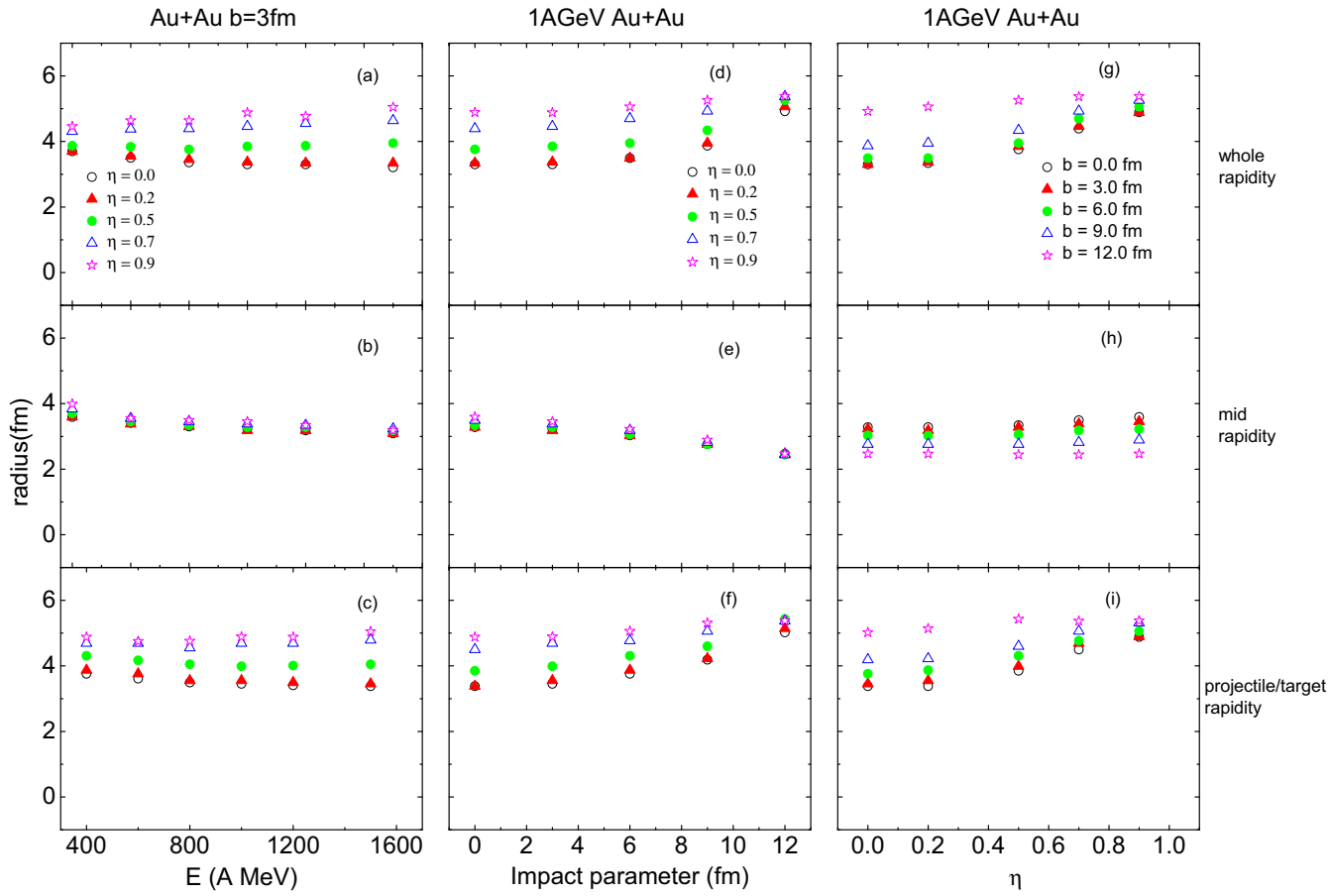

FIG. 4. Gaussian source radius as a function of the incident energy for different η factors at fixed impact parameter $b = 3$ fm (left column), as a function of impact parameter with different η factors (middle column), and as a function of in-medium nucleon-nucleon cross-section reduction factor at different impact parameter (right column). From top to bottom are the Gaussian radius of free protons emitted from the whole-rapidity window, the mid-rapidity window, and the target or projectile rapidity window, respectively.

parameter. With increasing impact parameters, the effective source size gets bigger because apparently the (target or projectile) spectator region gets bigger and bigger with increasing impact parameter, and this effect is more pronounced if the in-medium decrease of the cross section is smaller. This indicates some geometrical effect and protons coming from spectator fragmentation mechanism. At the same time, the source size increases with the decreasing of the in-medium *NN* cross section (i.e., larger η factor). The smaller the impact parameter, the stronger the dependence of the source size on the in-medium *NN* cross section, which can be understood as a more frequent collision effect that is expected to affect the dynamical evolution. However, for correlation between protons from the mid-rapidity region, the tendency of the source size becomes decreasing with the increasing of impact parameter, regardless of the in-medium nucleon-nucleon cross section. This reverse dependence of source radius between mid-rapidity protons and projectile or target rapidity protons as a function of impact parameter indicates some geometrical evolution of participant and spectator regions, which can be also well seen from Fig. 3(b).

We should mention that to extract the above source size, theoretical calculations for C_{pp} were performed by using the Lednický-Lyuboshitz analytical method. The best fitting source size is judged by finding the minimum of the reduced χ-square. Figure 5 presents examples of the χ^2-variance between the IQMD calculations with the Lednický-Lyuboshitz analytical formalism and the Gaussian source correlation as a function of the radius of the Gaussian source in different impact parameters with the changing η factors [Figs. 5(a)–5(d)] or in different η factors with the changing impact parameters [Figs. 5(e)–5(h)]. Generally, the minimum can be well defined, but the errors on its location are apparently rather asymmetric.

Mid-rapidity protons are possibly experienced by the collective radial flow expansion in comparison with the projectile or target rapidity protons. To demonstrate how large the radial flow is for the mid-rapidity protons, we use the blast-wave (BW) fits to p_T spectra of protons in the mid-rapidity region. Here, we get the α value equal to $1/3$ on the p_T spectra of central collisions and fix this value when we do the fitting on the other impact parameters [60]. Figure 6 shows the p_T spectra of mid-rapidity protons in different incident energy for $b = 3$ fm and $\eta = 0.2$ [Fig. 6(a)], in different impact parameter for $E = 1A$ GeV and $\eta = 0.2$ [Fig. 6(b)], and with different in-medium cross section for $b = 3$ fm and $1A$ GeV [Fig. 6(c)], where the solid symbols represent the calculated results from

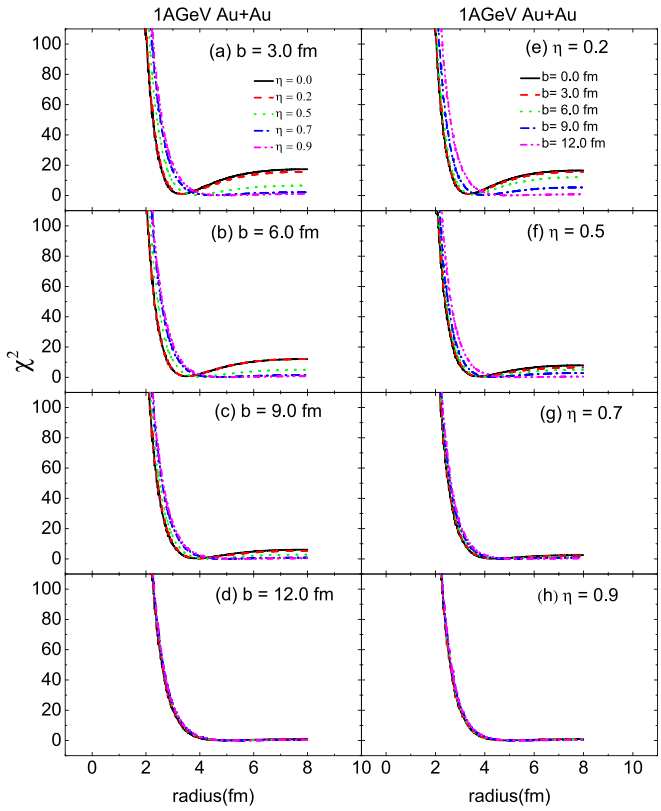

FIG. 5. The χ-square obtained from the fits of the proton-proton momentum correlation function by the Lednický *et al.* analytical formalism calculation as a function of the radius of the Gaussian source. (a)–(d) Each panel represents different fixed impact parameters with different η factor; (e)–(h) each panel represents different fixed η factors at different impact parameters.

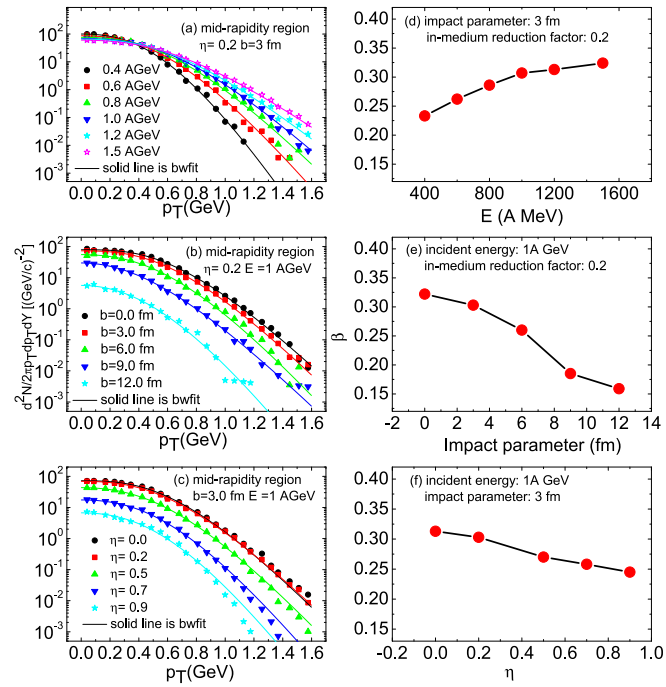

FIG. 6. (a)–(c) Blast-wave fitting to p_T spectra of protons in the mid-rapidity region: (a) incident energy dependence for $b = 3$ fm and $\eta = 0.2$, (b) impact parameter dependence at $E = 1A$ GeV and $\eta = 0.2$, and (c) in-medium cross-section dependence at $b = 3$ fm and $1A$ GeV. (d)–(f) The fitted radial flow parameter (β) as a function of (d) beam energy, (e) impact parameter at $1A$ GeV and $\eta = 0.2$, and (f) in-medium cross-section reduction factor at $1A$ GeV and $b = 3$ fm.

the IQMD model and the solid lines are the BW fits. Overall all lines can well reproduce the spectra, from which the radial flow parameters can be systematically extracted. Figure 6 also displays the extracted radial flow parameters (β) as a function of incident energy at $b = 3$ fm and $\eta = 0.2$ [Fig. 6(d)], as a function of impact parameter at $E = 1A$ GeV and $\eta = 0.2$ [Fig. 6(e)], and as a function of in-medium cross-section factor at $E = 1A$ GeV and $b = 3$ fm [Fig. 6(f)]. Obviously, the radial flow becomes stronger in higher incident energy as well as in more central collisions. Meanwhile, the larger in-medium nucleon-nucleon cross section (i.e., smaller η values) leads to larger radial flow due to the frequent nucleon-nucleon collision in the overlap zone. It is noticed that radial flow was already extensively discussed in intermediate- and high-energy HIC (e.g., by Helgesson *et al.* [63]).

For mid-rapidity *p-p* correlation, let us have a close look at correlation strength versus the radial flow. Since we have the relationship between the correlation strength at 20 MeV/c ($C_{pp}(q = 20\,\mathrm{MeV}/c)$) versus beam energy as well as the radial flow (β) versus beam energy, we can obtain the relationship between $C_{pp}(q = 20$ MeV/$c)$ and β which is displayed in Fig. 7(a) in the condition of $b = 3$ fm and $\eta = 0.2$. It tells us that the larger the radial flow velocity, the stronger the proton-proton correlation. In the same way, we got $C_{pp}(q =$ 20 MeV/c) versus β in Fig. 7(b) in the condition of $E = 1A$ GeV and $\eta = 0.2$ where the impact parameter is a variable. In this case, anti-correlation is observed. Similarly, $C_{pp}(q =$ 20 MeV/c) versus β is shown in Fig. 7(c) in the condition of $E = 1A$ GeV and $b = 3$ fm where the in-medium nucleon-nucleon cross-section reduction factor is a variable. Here, a slight increasing behavior is demonstrated. Seen from the above three variables, we found no unique dependence of *p-p* correlation function as a function of radial flow parameter.

IV. SUMMARY

In the present work, we use the IQMD transport approach to calculate the phase-space points at the freeze-out stage for Au + Au collisions from 0.4 to 1.5A GeV. Afterwards the phase-space points were processed within the Lednický-Lyuboshitz analytical formalism to reconstruct the proton-proton correlation function. In this way, we systematically study how the in-medium NN cross section affects the strength of the momentum correlation function of proton-proton pairs for Au + Au from 0.4 to 1.5A GeV in different rapidity windows and different impact parameters. Results show that the larger in-medium NN cross section results in a stronger momentum correlation function than a smaller in-medium NN cross section, especially at small impact parameters, for the whole rapidity or projectile or target rapidity proton pairs. This behavior is interpreted as a stronger correlation

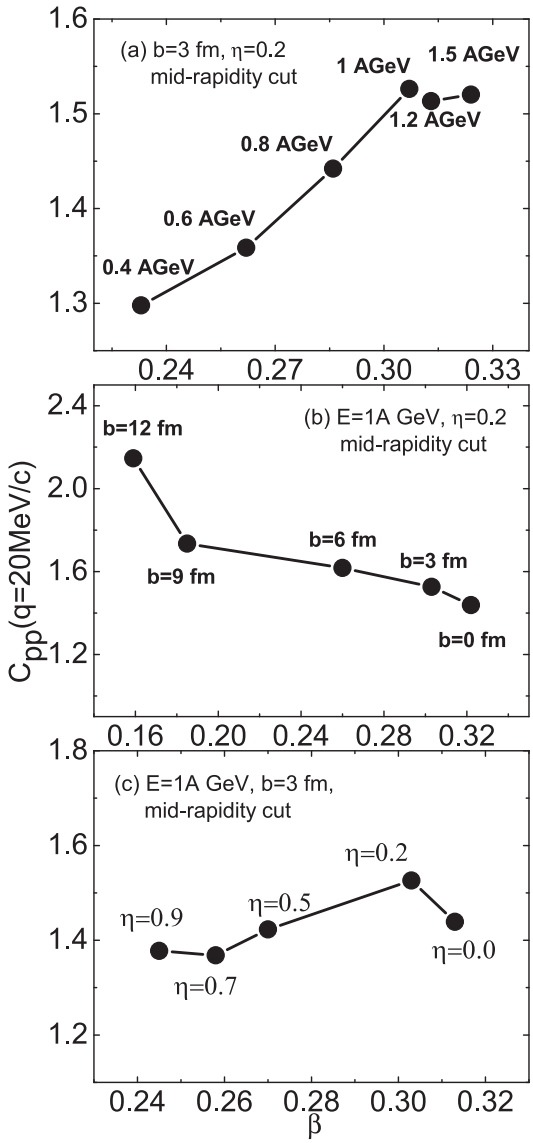

FIG. 7. Correlation strength at $q = 20\,\mathrm{MeV}/c$ as a function of the radial flow parameter (β) in different conditions. (a) Beam energy is a variable as shown in figure, at fixed $b = 3$ fm and $\eta = 0.2$; (b) impact parameter is a variable as shown in figure, at fixed $E = 1A$ GeV and $\eta = 0.2$; and (c) the in-medium nucleon-nucleon cross-section reduction factor is a variable as shown in figure, at fixed $E = 1A$ GeV and $b = 3$ fm.

for equilibrium-like protons induced by the higher nucleon-nucleon collision rate. However, for the mid-rapidity proton emission, the in-medium nucleon-nucleon cross section has less effect on the momentum correlation function due to a very different emission mechanism. In addition, the impact parameter effect on the HBT strength was also addressed in the work. We showed that the HBT strength has a very different dependence between the whole rapidity or projectile or target rapidity proton pairs and the mid-rapidity proton pairs. For proton pairs from the projectile or target rapidity, it decreases with the increasing of impact parameter, but for proton pairs from mid-rapidity, it increases with the increasing of impact parameter. By fitting the momentum correlation function with the Gaussian source, the effective proton emission source sizes are extracted. Results show that the source radius generally increases with the increasing of the impact parameter for emitted protons within the whole rapidity or projectile (target) rapidity; however, it decreases versus the impact parameter for the mid-rapidity protons and it shows insensitivity to the in-medium nucleon-nucleon cross section. The above phenomenon reflects the evolution of source size with the collision geometry; i.e., the mid-rapidity source becomes smaller but the projectile or target source becomes larger with the increasing of impact parameter. Moreover, the beam energy dependence of the HBT strength is also presented. Generally, the HBT strength shows a slight change with beam energy especially for the whole-rapidity or projectile (target) rapidity proton pairs. By using the blast-wave fits to the transverse momentum spectra of mid-rapidity protons, the radial flow parameters are systemically extracted as a function of beam energy, impact parameter, and in-medium nucleon-nucleon reduction factor, and therefore relationships of HBT strength versus radial flow parameter are constructed in different conditions. However, no unique dependence is found, which indicates the radial flow is not a decisive variable for the p-p correlation.

ACKNOWLEDGMENTS

This work was supported partly by the National Natural Science Foundation of China under Contracts No. 11421505 and No. 11220101005, the Major State Basic Research Development Program in China under Contract No. 2014CB845401, and the Key Research Program of Frontier Sciences of the CAS under Grant No. QYZDJ-SSW-SLH002.

[1] R. Hanbury Brown and R. Q. Twiss, Nature (London) **178**, 1046 (1956).
[2] G. Goldhaber *et al.*, Phys. Rev. **120**, 300 (1960).
[3] H. Boal, C. K. Gelbke, and B. K. Jennings, Rev. Mod. Phys. **62**, 553 (1990).
[4] U. Heinz and B. Jacak, Annu. Rev. Nucl. Part. Sci. **49**, 529 (1999); U. A. Wiedemann and U. Heinz, Phys. Rep. **319**, 145 (1999).
[5] N. A. Orr, Nucl. Phys. A **616**, 155 (1997).
[6] X. G. Cao, X. Z. Cai, Y. G. Ma, D. Q. Fang, G. Q. Zhang, W. Guo, J. G. Chen, and J. S. Wang, Phys. Rev. C **86**, 044620 (2012).
[7] K. Ieki *et al.*, Phys. Rev. Lett. **70**, 730 (1993); F. M. Marques *et al.*, Phys. Lett. B **476**, 219 (2000).
[8] M. T. Yamashita, T. Frederico, and L. Tomio, Phys. Rev. C **72**, 011601(R) (2005); M. Petrascu *et al.*, *ibid.* **69**, 011602(R) (2004).
[9] Z. Kohley *et al.*, Phys. Rev. Lett. **110**, 152501 (2013); E. Lunderberg *et al.*, *ibid.* **108**, 142503 (2012).
[10] P. Zhou *et al.*, Int. J. Mod. Phys. E **19**, 957 (2010); X. Y. Sun *et al.*, *ibid.* **19**, 1823 (2010).
[11] Y. G. Ma *et al.*, Phys. Lett. B **743**, 306 (2015).
[12] D. Q. Fang *et al.*, Phys. Rev. C **94**, 044621 (2016).

[13] Y. B. Wei *et al.*, Phys. Lett. B **586**, 225 (2004); J. Phys. G **30**, 2019 (2004).
[14] S. Pratt and M. B. Tsang, Phys. Rev. C **36**, 2390 (1987).
[15] J. P. Sullivan *et al.*, Phys. Rev. Lett. **70**, 3000 (1993).
[16] W. Bauer, C. K. Gelbke, and S. Pratt, Annu. Rev. Nucl. Part. Sci. **42**, 77 (1992).
[17] C. Adler *et al.* (STAR Collaboration), Phys. Rev. Lett. **87**, 082301 (2001); J. Adams *et al.* (STAR collaboration), *ibid.* **93**, 012301 (2004); Phys. Rev. C **71**, 044906 (2005); S. S. Adler *et al.* (PHENIX Collaboration), Phys. Rev. Lett. **93**, 152302 (2004); B. Abelev *et al.* (STAR Collaboration), Phys. Rev. C **80**, 024905 (2009); **81**, 024911 (2010).
[18] K. Aamodt *et al.* (ALICE Collaboration), Phys. Lett. B **696**, 328 (2011).
[19] L. Adamczyk *et al.* (STAR Collaboration), Nature (London) **527**, 345 (2015).
[20] Z. Q. Zhang, Ph.D. dissertation, Shanghai Institute of Applied Physics, Chinese Academy of Sciences, 2017 (unpublished).
[21] H. Q. Zhang, Nat. Sci. Rev. **3**, 154 (2016).
[22] Z.-Q. Zhang and Y.-G. Ma, Nucl. Sci. Techniques **27**, 152 (2016).
[23] Z.-Q. Zhang, S. Zhang, and Y.-G. Ma, Chin. Phys. C **38**, 014102 (2014).
[24] Z.-W. Lin, C. M. Ko, and S. Pal, Phys. Rev. Lett. **89**, 152301 (2002); J. Phys. G: Nucl. Part. Phys. **30**, S263 (2004).
[25] F. Retiére and M. A. Lisa, Phys. Rev. C **70**, 044907 (2004).
[26] M. A. Lisa, Acta Phys. Pol. B **47**, 1847 (2016).
[27] J. Yang and W.-N. Zhang, Nucl. Sci. Techniques **27**, 147 (2016).
[28] R. Ghetti *et al.*, Phys. Rev. Lett. **91**, 092701 (2003); G. Verde *et al.*, Eur. Phys. J. A **30**, 81 (2006).
[29] W. G. Gong, W. Bauer, C. K. Gelbke, and S. Pratt, Phys. Rev. C **43**, 781 (1991).
[30] Y. G. Ma *et al.*, Phys. Rev. C **73**, 014604 (2006).
[31] N. Colonna *et al.*, Phys. Rev. Lett. **75**, 4190 (1995).
[32] R. Ghetti *et al.*, Phys. Rev. C. **69**, 031605(R) (2004).
[33] L. W. Chen, V. Greco, C. M. Ko, and B. A. Li, Phys. Rev. Lett. **90**, 162701 (2003).
[34] M. Lv, Y. G. Ma, J. H. Chen, D. Q. Fang, and G. Q. Zhang, Phys. Rev. C **95**, 024614 (2017).
[35] B. ter Haar and R. Malfliet, Phys. Rev. C **36**, 1611 (1987); G. Q. Li and R. Machleidt, *ibid.* **48**, 1702 (1993).
[36] Cai Xiangzhou, Feng Jun, Shen Wenqing, Ma Yugang, Wang Jiansong, and Ye Wei, Phys. Rev. C **58**, 572 (1998); J.-Y. Liu, W.-J. Guo, S.-J. Wang, W. Zuo, Q. Zhao, and Y.-F. Yang, Phys. Rev. Lett. **86**, 975 (2001).
[37] Y. Zhang, Z. Li, and P. Danielewicz, Phys. Rev. C **75**, 034615 (2007); B. Chen, F. Sammarruca, and C. A. Bertulani, *ibid.* **87**, 054616 (2013).
[38] R. Lednicky and V. L. Lyuboshitz, Sov. J. Nucl. Phys. **35**, 770 (1982).
[39] R. Lednicky, Phys. At. Nucl. **71**, 1572 (2008).
[40] R. Lednicky, Phys. Part. Nucl. **40**, 307 (2009).
[41] S. E. Koonin, Phys. Lett. B **70**, 43 (1977).
[42] R. Lednicky and V. L. Lyuboshitz, Heavy lon Phys. **3**, 93 (1996).
[43] P. Danielewicz, Phys. Lett. B **146**, 168 (1984).
[44] J. Aichelin, A. Rosenhauer, G. Peilert, H. Stoecker, and W. Greiner, Phys. Rev. Lett. **58**, 1926 (1987).
[45] T. Z. Yan *et al.*, Phys. Lett. B **638**, 50 (2006).
[46] Y. G. Ma and W. Q. Shen, Phys. Rev. C **51**, 710 (1995).
[47] G. Q. Zhang *et al.*, Phys. Rev. C **84**, 034612 (2011); Y. Z. Xing *et al.*, Chin. Phys. Lett. **33**, 122501 (2016).
[48] Z. Q. Feng, Nucl. Sci. Techniques **29**, 40 (2018).
[49] C. L. Zhou, Y. G. Ma, D. Q. Fang, G. Q. Zhang, J. Xu, X. G. Cao, and W. Q. Shen, Phys. Rev. C **90**, 057601 (2014).
[50] C. Tao, Y. G. Ma, G. Q. Zhang *et al.*, Nucl. Sci. Techniques **24**, 030502 (2013); C. Tao, Y. G. Ma, G. Q. Zhang, X. G. Cao, D. Q. Fang, and H. W. Wang, Phys. Rev. C **87**, 014621 (2013).
[51] J. Chen, Z.-Q. Feng, and J.-S. Wang, Nucl. Sci. Techniques **27**, 73 (2016).
[52] B. S. Huang and Y. G. Ma, Chin. Phys. Lett. **34**, 072401 (2017).
[53] W. J. Xie and F. S. Zhang, Chin. Phys. Lett. **32**, 122502 (2015).
[54] T. T. Wang *et al.*, Chin. Phys. Lett. **32**, 062501 (2015).
[55] C. Hartnack, Rajeev K. Puri, J. Aichelin, J. Konopka, S. A. Bass, H. Stöcker, and W. Greiner, Eur. Phys. J. A **1**, 151 (1998).
[56] K. Chen *et al.*, Phys. Rev. **166**, 949 (1968).
[57] E. Fermi, Theor. Phys. **5**, 570 (1950).
[58] P. J. Siemens and J. O. Rasmussen, Phys. Rev. Lett. **42**, 880 (1979).
[59] J. P. Bondorf, S. I. A. Garpman, and J. Zimányi, Nucl. Phys. A **296**, 320 (1978).
[60] M. Lv, Y. G. Ma, G. Q. Zhang, J. H. Chen, and D. Q. Fang, Phys. Lett. B **733**, 105 (2014).
[61] E. Schnedermann, J. Sollfrank, and U. Heinz, Phys. Rev. C **48**, 2462 (1993).
[62] S. Zhang, Y. G. Ma, J. H. Chen, and C. Zhong, Adv. High Energy Phys. **2016**, 9414239 (2016).
[63] J. Helgesson, T. Csörgö, M. Asakawa, and B. Lörstad, Phys. Rev. C **56**, 2626 (1997).